nature geoscience

LETTERS

PUBLISHED ONLINE: 22 JUNE 2014 | DOI: 10.1038/NGEO2186

Externally forced fluctuations in ocean temperature at Greenland glaciers in non-summer months

Rebecca H. Jackson[1,2*], Fiammetta Straneo[1] and David A. Sutherland[3]

Enhanced submarine melting of outlet glaciers has been identified as a plausible trigger for part of the accelerated mass loss from the Greenland ice sheet[1–3], which at present accounts for a quarter of global sea level rise[4]. However, our understanding of what controls the submarine melt rate is limited and largely informed by brief summer surveys in the fjords where glaciers terminate. Here, we present continuous records of water properties and velocity from September to May in Sermilik Fjord (2011–2012) and Kangerdlugssuaq Fjord (2009–2010), the fjords into which the Helheim and Kangerdlugssuaq glaciers drain. We show that water properties, including heat content, vary significantly over timescales of three to ten days in both fjords. This variability results from frequent velocity pulses that originate on the shelf outside the fjord. The pulses drive rapid water exchange with the shelf and renew warm water in the fjord more effectively than any glacial freshwater-driven circulation. Our observations suggest that, during non-summer months, the glacier melt rate varies substantially and depends on externally forced ocean flows that rapidly transport changes on the shelf towards the glaciers' margins.

The submarine melt rate depends on near-glacier ocean temperature and circulation[5]. Recent studies assume that both these things are governed by the glacier's freshwater inputs[6–10], and that other drivers, such as tides, air–sea fluxes and shelf-driven exchange, can be neglected. In this prevailing framework, submarine meltwater and subglacial discharge (surface meltwater draining at the glacier's base) form buoyant plumes, entrain ambient water and drive an overturning circulation that transports shelf waters towards the glacier. Under this assumption, enhanced subglacial discharge increases ocean heat transport, submarine melting and the renewal of near-glacier waters[6–8].

However, the extent to which the glacier-driven circulation influences the renewal of warm water in these fjords is unclear. Limited velocity data indicates that shelf variability may play an important role in driving fjord flows[10–12], although conclusive evidence is absent. Furthermore, most observational studies rely on brief, summer surveys[2,10,13–17] that offer limited insight into drivers of summer variability and no information about non-summer months.

Here, we present new insight into fjord dynamics from moored records in Sermilik and Kangerdlugssuaq fjords (Fig. 1a), where Helheim and Kangerdlugssuaq glaciers (the fifth and third largest outlets of the Greenland ice sheet, respectively[18]) deposit freshwater as submarine meltwater, subglacial discharge, surface runoff and icebergs. The vertical calving fronts of both glaciers ground ~600 m below sea level at the head of their respective fjords (~70/100 km long and ~6 km wide)[19], which connect the glaciers to the continental shelf. The predominant water masses of Greenland's southeast shelf form a two-layer structure within Sermilik Fjord[11,20]: cold, fresh Polar-origin water (PW) overlying warm, salty Atlantic-origin water (AW), with some modification due to glacial inputs[16]. A similar water mass structure is found in Kangerdlugssuaq, with an additional dense Atlantic water mass originating in the Nordic Seas[19]. In both Sermilik and Kangerdlugssuq fjords, the shallowest sills (at 530 and 550 m, respectively) are well below the AW/PW interface[13,21,22], allowing relatively unimpeded exchange between the fjord and shelf (Fig. 1a,b). The shelf region of southeast Greenland outside both fjords is characterized by frequent, strong, along-shore winds[23] and fast ocean currents[20].

Winds and subglacial discharge—two potential drivers of fjord circulation—exhibit a strong seasonality in this region. From September through May, shelf winds are strong along Greenland's southeast coast[23], and subglacial discharge is negligible as air temperatures drop below freezing[24]. During summer, winds weaken, and subglacial discharge increases, becoming a larger freshwater source than submarine melt[24]. This seasonality probably modulates the glacier-driven circulation and submarine melt rate; one modelling study estimated the summer melt rate at Helheim Glacier to be twice the non-summer rate as a result of variations in subglacial discharge[7]. According to this scaling, nevertheless, 60% of the annual submarine melt would occur in non-summer months, an important but unstudied period.

Extensive oceanic water property and velocity records (Methods) were collected during non-summer months in 2011–2012 from Sermilik Fjord and the adjacent shelf (Fig. 1a–d) and in 2009–2010 from Kangerdlugssuaq Fjord (excluding velocity, Fig. 1a,e).

In Sermilik Fjord, the records indicate that AW and PW are always present, but their properties and thicknesses vary over timescales of hours to months (Fig. 1d). The upper water column near the AW/PW interface exhibits the largest variability, a result of seasonal trends[11]—for example, PW deepening and cooling in the winter—and higher frequency fluctuations in the interface's depth, often exceeding 50 m over several days (Fig. 1d). Within the AW layer, temperature ranges from 2 °C to 5.2 °C and exhibits transient fluctuations (typically 0.3–0.7 °C) that last several days, as well as more sustained shifts, such as an abrupt cooling in late March. Significant variability exists even at 851 m, well below sill depth.

The fjord's persistent stratification and occasional increases in heat content preclude internal mixing (which would reduce stratification and redistribute heat) or surface fluxes (which would

[1]Department of Physical Oceanography, Woods Hole Oceanographic Institution, Woods Hole, Massachusetts 02543, USA, [2]Department of Earth, Atmospheric and Planetary Sciences, Massachusetts Institute of Technology, Cambridge, Massachusetts 02139, USA, [3]Department of Geological Sciences, University of Oregon, Eugene, Oregon 97403, USA. *e-mail: rjackson@whoi.edu

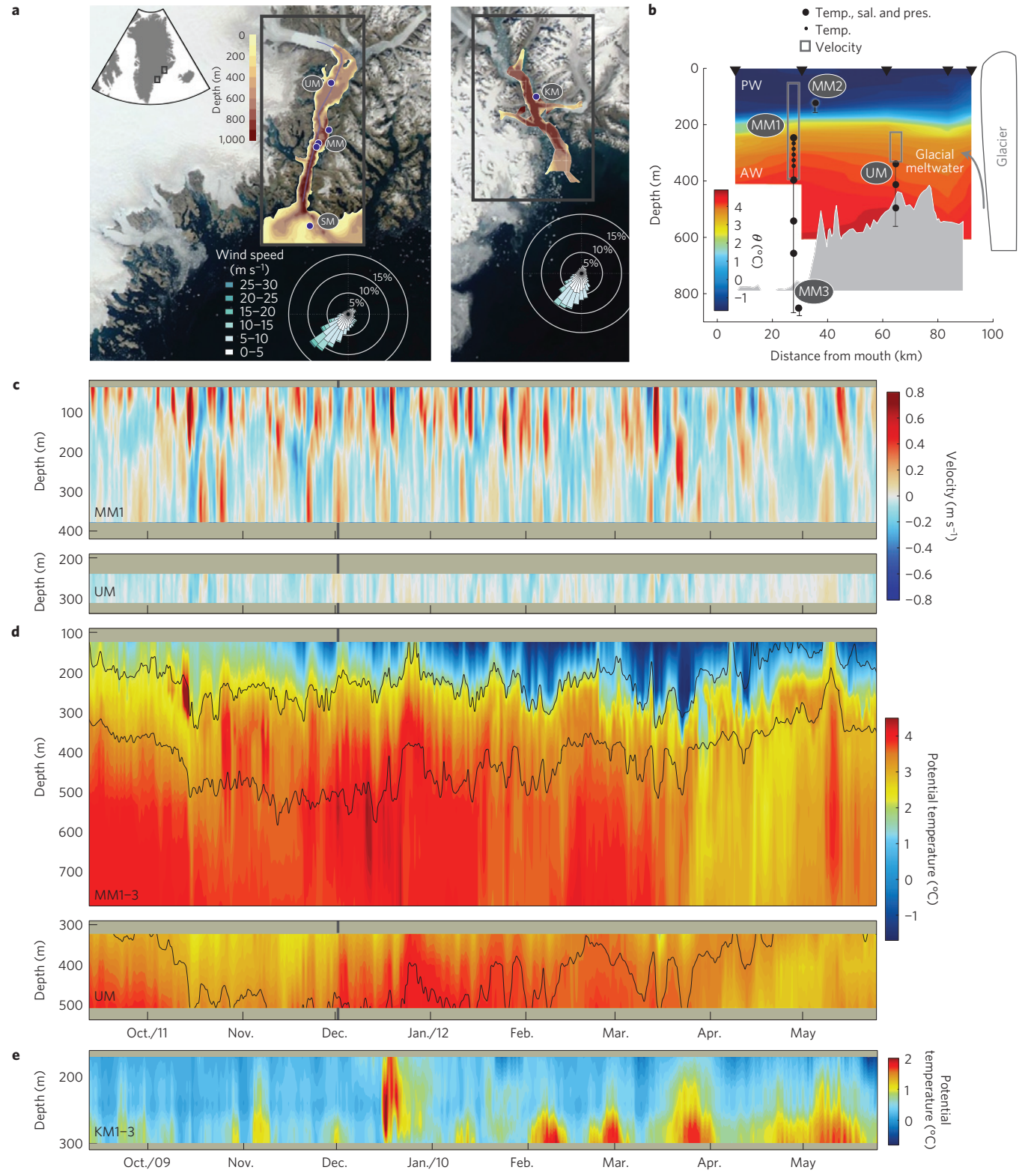

Figure 1 | Large, rapid variations in velocity and water properties observed in two glacial fjords. a, Satellite images of Sermilik and Kangerdlugssuaq fjords with bathymetry overlaid. Circles indicate mooring locations and the line shows the path of the along-fjord Sermilik profile in **b**. Wind roses of speed and direction on the shelf are from ERA-Interim Reanalysis from 2009 to 2013 (Methods). **b**, Along-fjord potential temperature from a 2010 winter survey of Sermilik[16] with a schematic of Sermilik moorings (mid-fjord moorings, MM1–3; upper-fjord, UM; shelf mooring is not shown), instruments and water masses. AW, Atlantic-origin water; PW, Polar-origin water. **c**, Along-fjord velocity in Sermilik at mid-fjord (MM1, top panel) and upper-fjord (UM, bottom) moorings, where positive indicates up-fjord flow towards the glacier. **d**, Potential temperature in Sermilik at mid-fjord (MM1–3, top panel) and upper-fjord (UM, bottom) moorings with contours of $\sigma_\theta = [27.0, 27.5]$ kg m^{-3} overlaid. **e**, Potential temperature in Kangerdlugssuaq at mid-fjord (KM1–3) for the same nine months but different years (2009–2010). All records are low-pass filtered with a fourth order 26-h Butterworth filter. The grey vertical lines in December in **c**,**d** mark an up-fjord flow in the lower layer that is highlighted in Fig. 2c,d.

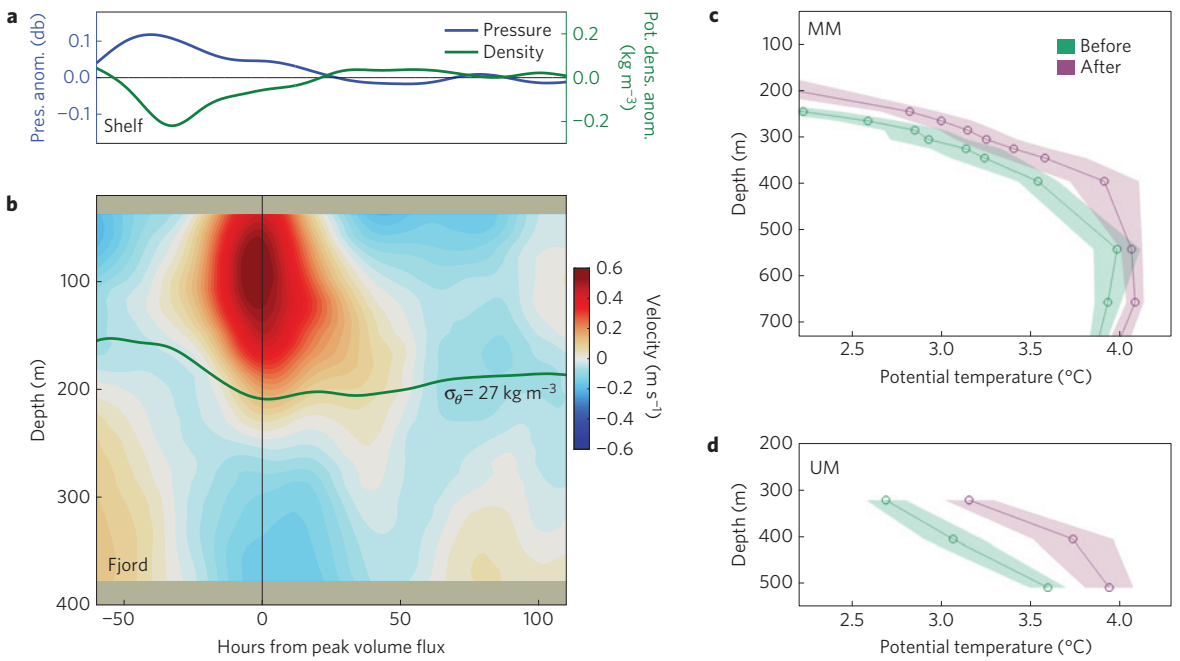

Figure 2 | Structure and impact of velocity pulses. a, Composites of potential density anomaly and bottom pressure anomaly (both 26-h low-pass filtered, with 30-day low-pass signal removed) from shelf mooring. **b**, Composite of velocity at mid-fjord with contour of $\sigma_\theta = 27.0\,\mathrm{kg\,m^{-3}}$ from composite of mid-fjord potential density (30-day low-pass signal removed and mean added back). Positive velocities indicate flow up-fjord, towards the glacier. The composites in **a**,**b** are of various records over the 16 strongest velocity pulses (defined by an up-fjord volume flux in the upper layer exceeding $3.7 \times 10^5\,\mathrm{m^3\,s^{-1}}$; Methods and Fig. 3a). **c**,**d**, Potential temperature profiles during four-day periods proceeding and following a strong up-fjord flow (indicated with grey vertical lines in Fig. 1c,d) in the AW layer at mid-fjord mooring (MM; **c**) and upper-fjord mooring (UM; **d**). Circles show average temperature at the instrument during each period; shading indicates the 95% range of all measurements over this period.

reduce stratification and cool) from being the primary drivers of these changes. Instead, we attribute the variability to rapid exchange with the shelf, driven by energetic, sheared flows in the along-fjord direction (Fig. 1c). These pulses last several days and frequently exceed $50\,\mathrm{cm\,s^{-1}}$ in the upper layer, with mid-fjord RMS velocities between 10 and $21\,\mathrm{cm\,s^{-1}}$ at all depths (much larger than the $\sim 2.5\,\mathrm{cm\,s^{-1}}$ RMS tidal component). Upper-fjord velocities are reduced but well correlated with mid-fjord flow (Supplementary Information).

The velocity typically reverses direction at the AW/PW interface (the pycnocline) and is faster in the upper layer. This structure is consistent with the first baroclinic dynamical mode, calculated from the fjord stratification, and the first empirical orthogonal function (EOF) of the mid-fjord velocity, which accounts for 67% of the variability. A similar mode had also been observed in summer synoptic surveys[12]. Flow in both layers typically reverses every few days, with a significant spectral peak at 4–10-day periods, or synoptic timescales (Supplementary Information).

We attribute these pulses to forcing from the shelf, through a pumping mechanism termed the intermediary circulation. Driven by density fluctuations at a fjord's mouth[25,26], this mechanism has been found to force more fjord/shelf exchange than tidal or estuarine flows in some Scandinavian fjords[27,28]. A previous summer study of Sermilik hypothesized that intermediary circulations may be important for flushing the fjord[11]; however, until now, no direct evidence of this mechanism or its associated variability existed.

Examination of the velocity pulses in our data reveals a structure consistent with intermediary circulation theory and strong shelf forcing. A composite of 16 events (Fig. 2a,b) illustrates the basic features of these pulses: the PW layer thickens, associated with depressed isopycnals, as a strong up-fjord flow develops above the interface and a weaker out-flow below. Velocity in each layer then reverses as the density field rebounds. These pulses originate on the shelf with a negative density anomaly and positive bottom pressure anomaly (indicating a positive sea-surface height anomaly) that propagate up-fjord at speeds approximately matching the first baroclinic and barotropic mode phase speeds, respectively (Supplementary Information).

All fjord velocity pulses are associated with shelf density fluctuations, and most are also preceded by along-shore, downwelling-favourable winds on the shelf that are typical of this region (Fig. 3). These winds depress isopycnals and raise the sea surface towards the coastline, resulting in the shelf/fjord set-up described above. A high coherence between shelf wind and shelf density at periods of two to ten days confirms this link (Fig. 3). Bottom pressure anomalies on the shelf and mid-fjord, equivalent to a $\sim$15 cm increase in surface height, accompany wind events and are consistent with on-shore transport from downwelling-favourable winds (Supplementary Information). We speculate that other phenomena (for example, coastally trapped waves, AW eddies) can generate shelf/fjord pressure gradients, forcing occasional pulses without associated winds.

These pulses drive significant exchange with the shelf over short timescales, causing high-frequency variability and abrupt shifts in fjord water properties. The average volume exchanged in each layer over the 16 strongest pulses is $8.5 \pm 0.8 \times 10^{10}\,\mathrm{m^3}$—equivalent to $\sim$50% of the average upper layer volume in the entire fjord, or $\sim$25% of the lower layer (Fig. 3c and Methods).

Regarding the glacier, these pulses significantly alter the fjord's heat content via changes in layer thickness and property shifts within layers. All pulses have a transient response from the first effect; for example, up-fjord flow in the PW layer thickens that layer, increasing the volume of PW relative to AW and decreasing the average water column temperature. Furthermore, shifts in AW temperature, such as the warming event shown in Fig. 2c,d, often coincide with lower layer in-flow as water is advected in

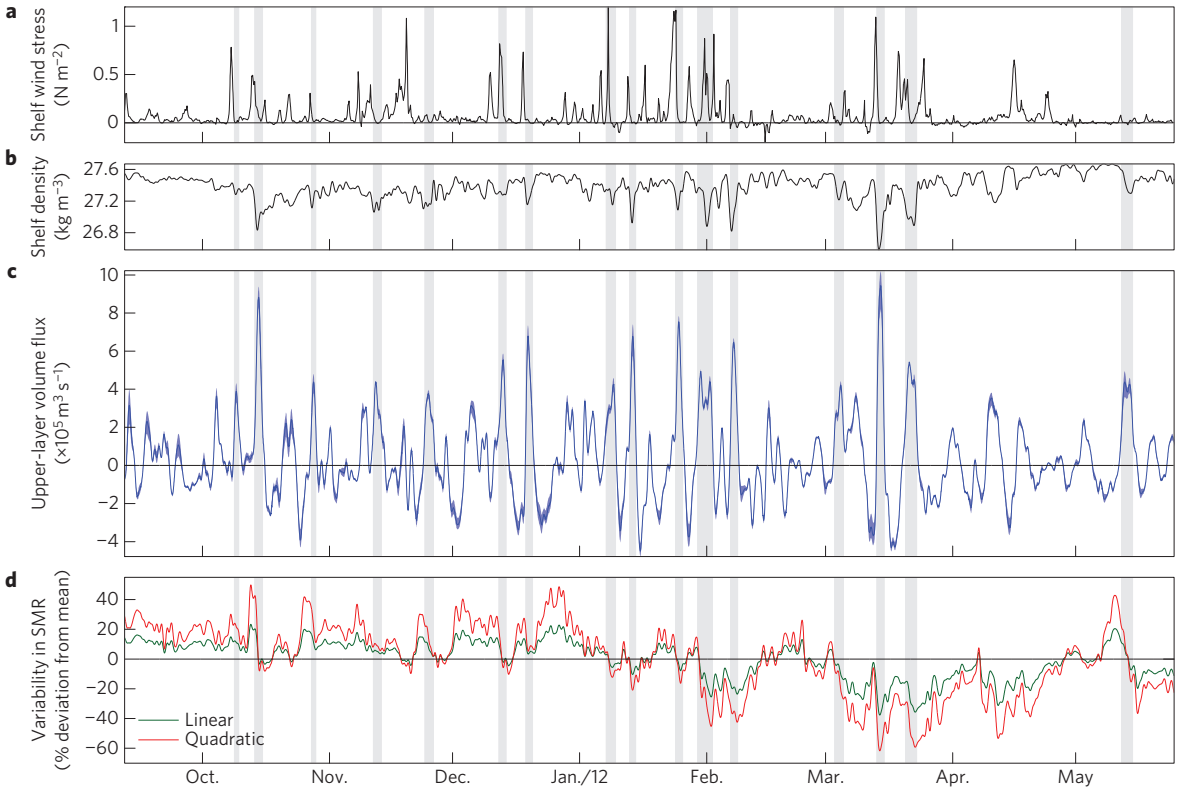

Figure 3 | Shelf-driven exchange and melt rate variability. a, Along-shore wind stress on the shelf outside Sermilik; positive winds are to the southwest, which is downwelling-favourable (Methods). **b**, Potential density from shelf mooring. **c**, Volume flux in upper layer at mid-fjord mooring, assuming uniform across-fjord velocity; positive indicates flow towards the glacier. **d**, Variability (as the percentage deviation from the mean) in submarine melt rate based on a linear or quadratic scaling law between melt rate and average water column temperature (Methods). Shading in all panels over the 16 strongest pulses, which were used for the composites in Fig. 2a,b.

from the shelf during energetic pulses. Changes in the average AW temperature (Methods) in the upper-fjord lag the mid-fjord by 26 h, suggesting a propagation speed of 0.4 m s^{-1}, which is consistent with advection by the observed velocity. All pulses drive transient changes in layer thickness and are associated with heaving isopycnals on the shelf. Only some pulses, however, advect new properties into the fjord, which, we argue, reflect changes in water properties on the shelf.

The mid-fjord water properties from Kangerdlugssuaq Fjord exhibit similar variability to Sermilik: high-frequency fluctuations (Fig. 1e), with a peak in energy and coherence between the density records at synoptic periods of 3–12 days. Without a shelf mooring outside Kangerdlugssuaq, we cannot directly attribute this variability to shelf forcing. However, significant coherence between fjord properties (density, pressure and temperature) and along-shore shelf winds at 6–11 day periods suggests that the same intermediary circulations are present and forced by along-shore shelf winds (Supplementary Information).

In summary, water properties and heat content within Sermilik and Kangerdlugssuaq fjords vary significantly on synoptic timescales throughout non-summer months. This variability is attributed to strongly sheared pulses driven by shelf density fluctuations, primarily due to along-shore winds. Individual events, lasting only several days, rapidly translate signals from the shelf to the upper fjord.

Our results have several important implications. The shelf-driven flow allows the fjords to track shelf variability on short timescales (days to weeks), as opposed to the longer timescales (months) associated with glacier-driven circulation, which we expect to have velocities of less than 2 cm s^{-1} in winter[7]. Although there must be a net export of freshwater from the glacier and import of heat for melting, the externally forced flow masks any signal of a glacier-driven flow in our nine-month records. The renewal and variability of AW does not seem to be controlled by glacial inputs for the majority of the year, reducing the possibility of a positive feedback between glacial meltwater and shelf exchange.

Our results also suggest that the submarine melt rate should vary significantly throughout non-summer months as a result of the observed fluctuations in temperature, which, we assume, are representative of property changes near the glacier. To estimate submarine melt variability, we rely on modelling studies that, in the absence of subglacial discharge, find melt to scale linearly or quadratically with ambient water temperature[7,8,29]. When we apply this scaling to our temperature observations in Sermilik Fjord, we find that the submarine melt rate would vary by ±20–50% of its mean value on synoptic timescales (Fig. 3d; Methods). These externally forced pulses might also change the kinetic energy at the ice boundary layer (and hence the submarine melt rate) or impact the ice mélange, which could affect glacier stability[30].

The scope of our results should be highlighted. We do not have records from the glacier/ocean boundary layer but from the 'far-field' ocean conditions that the glacier experiences. The velocity pulses and property variability at our moorings, however, suggest that the observed fluctuations penetrate far into the fjord. Rather than resolving processes at the glaciers' margins, our results provide the first non-summer oceanic boundary conditions one might use to force a glacier model. Additionally, we speculate that the fjord dynamics will be different in the summer months. When subglacial discharge increases and winds weaken, we expect

a competition between shelf-driven and glacier-driven flows, although the nature of their interaction is at present unclear. Helheim and Kangerdlugssuaq glaciers are two of the Greenland ice sheet's largest outlets, contributing 20% of the current ice sheet discharge anomaly[18], and their dynamics alone are worth understanding. We also expect, however, our results from Sermilik and Kangerdlugssuaq fjords to be applicable to other fjords around Greenland, although the magnitude of the intermediary flow will depend on the shelf variability and sill depth.

Methods

Moorings. In the Sermilik region, we deployed five moorings (SM, MM 1–3 and UM; locations in Fig. 1) to measure velocity in the fjord and water properties in the fjord and on the shelf. An upward-facing 75 kHz Acoustic Doppler Current Profiler (ADCP) on MM-1 measured velocity in 10 m bins between 388 m and the surface from August 2011 through to June 2012. The upper three bins (centred at 28, 18 and 8 m) were discarded owing to side-lobe contamination. An upward-facing 300 kHz ADCP on UM measured velocity in 8 m bins between 313 and 233 m from August 2011 to September 2012. Both instruments measured 10-min averaged velocity every hour. Gaps in the records—often from instrument contamination (for example, icebergs) or low-backscatter—were filled by removing a tidal fit, interpolating linearly, and adding back the tidal component. The along-fjord velocity was determined by rotating the velocity field into its principal axes and extracting the component along the major axis, which falls parallel to local bathymetry at both locations (32° and 35° from north at MM-1 and UM, respectively). The across-fjord velocities along the minor axis were smaller (with variance ~90% smaller than along-fjord variance) and are not discussed here.

Concurrently, nine conductivity-temperature-pressure sensors (Seabird SBE 37SMs and RBR XR-420s at 291 m on SM, 125, 246, 396, 542, 657 and 851 m on MM 1–3 and 323, 406 and 510 m on UM) and five temperature sensors (Onset Tidbit v2 at 266, 286, 306, 326 and 346 m on MM 1–3) recorded water properties. All temperature records from the mid-fjord moorings, MM 1–3, were combined to make the depth versus time contour plots in Fig. 1d, thereby neglecting horizontal variability between the nearby moorings. This approximation is supported by many synoptic surveys of the fjord and moored records, which show that the horizontal spatial variability within several kilometres is small compared with the variability in depth and time. Hydrographic surveys of the fjord were conducted on mooring deployment and recovery and used to calibrate the moored instruments.

In Kangerdlugssuaq, we deployed three mid-fjord moorings (KM1–3) from August 2009 to September 2010. Two temperature-conductivity-depth sensors (RBR XR-420s) were deployed at 166 m and 225 m on KM1 and KM2, respectively. KM3 was equipped with a depth recorder (RBR DR-1050) at 223 m and seven temperature sensors (Onset Tidbit v2) at 223, 243, 253, 263, 273, 283 and 303 m depths.

Wind. The ERA-Interim reanalysis, deemed successful at capturing winds on the shelf of southeast Greenland[23], is used to assess the shelf wind field (http://apps.ecmwf.int/datasets/data/interim_full_daily/). Outside of Sermilik and Kangerdlugssuaq fjords, the velocity component along the principal axis (230° and 210° from north, respectively) at a point 45 km offshore of each fjord's mouth was extracted for an along-shore wind time-series (Fig. 3a; locations shown by wind roses in Fig. 1a). By this convention, downwelling-favourable winds from the northeast are positive.

Volume flux. To calculate volume fluxes in Sermilik, we assume that the mid-fjord velocity field is uniform across the width of the fjord at the mooring location. Based on previous studies of lowered ADCP and CTD sections, there is some lateral shear, but to first order we neglect this variability[12,16]. Volume flux in the upper layer is defined as $Q=\sum_{i=1}^{n} v_i Wh$, where h equals 10 m, the depth range of each bin; W equals 7.5 km, the approximate width the fjord at the mooring location; n is the last bin above the AW/PW interface. This interface was chosen to be the 1,027 kg m^{-3} potential density contour from the 30-day high-pass filtered density field. The velocity record excludes the top 33 m of the water column, so four methods are used to extend the velocity profile to the surface and put an error estimate on the volume flux (Fig. 3). The surface velocities were filled in with: (1) a constant value equal to the top bin; (2) an extension of the mean shear observed in the depth range 33–73 m; (3) a linear shear such that the velocity goes to zero at the surface; (4) no velocity. The lower layer volume flux was not directly calculated because the velocity record ends at 400 m; however, we can infer it to be of approximately equal magnitude and opposite direction to the upper layer flux based on our knowledge of the density profile and presumed conservation of fjord volume. The upper layer volume flux was time-integrated over a pulse to determine the total volume exchanged, which was then compared to each layer's total volume in the fjord based on a mean interface depth of 180 m. Average volume exchanged during a pulse is compared to the total volume of each layer, although the fraction of water exchanged would be ~20% higher if compared to the volume of each layer upstream of the mooring (that is, between the mooring and the glacier).

Composites. Composites of the mid-fjord velocity, mid-fjord density, shelf density and shelf pressure were created by averaging these fields over the 16 strongest velocity pulses. These events were defined by an up-fjord volume flux (26-h low-pass filtered) in the upper layer exceeding 3.7×10^5 m^3 s^{-1} and aligned by the time of peak volume flux. The pulses are identified with grey shading in Fig. 3a.

Average AW temperature. To compare AW layer properties at different locations, the potential temperature records at MM and UM were each linearly interpolated onto a 10-m vertical grid and averaged between 350 and 530 m.

Melt rate deviations. We calculated a depth-averaged water column temperature by linearly interpolating our temperature records from MM onto a 10-m vertical grid and averaging between 125 m and 530 m. This depth range was chosen to best represent the water column in direct contact with the glacier (above the 530 m sill in the upper fjord) to the extent that we could resolve without extrapolation. Although we neglect the upper 125 m, we also know that the PW is close to the freezing temperature in winter and probably does not contribute significantly to submarine melting. We used this depth-averaged temperature to estimate the variability in the submarine melt rate (SMR), assuming a linear or quadratic relationship between the melt rate and the temperature: SMR $\propto(T-T_f)$ or SMR $\propto(T-T_f)^2$, where T is the average water column temperature and T_f is the freezing temperature. By this scaling, the deviation in the submarine melt rate (from its time-mean value) would be:

$$\mathrm{PDS}=\frac{\mathrm{SMR}-\overline{\mathrm{SMR}}}{\overline{\mathrm{SMR}}}\times100=\frac{(T-T_f)-\overline{(T-T_f)}}{\overline{(T-T_f)}}\times100\ \text{(linear)}$$

$$=\frac{(T-T_f)^2-\overline{(T-T_f)^2}}{\overline{(T-T_f)^2}}\times100\ \text{(quadratic)}$$

where PDS is the percentage deviation about the mean submarine melt rate.

Received 17 March 2014; accepted 16 May 2014; published online 22 June 2014

References

1. Thomas, R. H. Force–perturbation analysis of recent thinning and acceleration of Jakobshavn Isbrae, Greenland. *J. Glaciol.* **50,** 57–66 (2004).
2. Holland, D. M., Thomas, R. H., de Young, B., Ribergaard, M. H. & Lyberth, B. Acceleration of Jakobshavn Isbræ triggered by warm subsurface ocean waters. *Nature Geosci.* **1,** 659–664 (2008).
3. Vieli, A. & Nick, F. M. Understanding and modelling rapid dynamic changes of tidewater outlet glaciers: Issues and implications. *Surv. Geophys.* **32,** 437–458 (2011).
4. Shepherd, A. *et al.* A reconciled estimate of ice-sheet mass balance. *Science* **338,** 1183–1189 (2012).
5. Jenkins, A., Nicholls, K. W. & Corr, H. F. J. Observation and parameterization of ablation at the base of Ronne Ice Shelf, Antarctica. *J. Phys. Oceanogr.* **40,** 2298–2312 (2010).
6. Xu, Y., Rignot, E., Menemenlis, D. & Koppes, M. Numerical experiments on subaqueous melting of Greenland tidewater glaciers in response to ocean warming and enhanced subglacial discharge. *Ann. Glaciol.* **53,** 229–234 (2012).
7. Sciascia, R., Straneo, F., Cenedese, C. & Heimbach, P. Seasonal variability of submarine melt rate and circulation in an East Greenland fjord. *J. Geophys. Res.* **118,** 2492–2506 (2013).
8. Jenkins, A. Convection-driven melting near the grounding lines of Ice Shelves and tidewater glaciers. *J. Phys. Oceanogr.* **41,** 2279–2294 (2011).
9. Motyka, R. J., Hunter, L., Echelmeyer, K. A. & Connor, C. Submarine melting at the terminus of a temperate tidewater glacier, LeConte Glacier, Alaska, USA. *Ann. Glaciol.* **36,** 57–65 (2003).
10. Rignot, E., Koppes, M. & Velicogna, I. Rapid submarine melting of the calving faces of West Greenland glaciers. *Nature Geosci.* **3,** 187–191 (2010).
11. Straneo, F. *et al.* Rapid circulation of warm subtropical waters in a major glacial fjord in East Greenland. *Nature Geosci.* **3,** 182–186 (2010).
12. Sutherland, D. A. & Straneo, F. Estimating ocean heat transports and submarine melt rates in Sermilik Fjord, Greenland, using lowered acoustic Doppler current profiler (LADCP) velocity. *Ann. Glaciol.* **53,** 50–58 (2012).

13. Inall, M. E. *et al.* Oceanic heat delivery via Kangerdlugssuaq Fjord to the south-east Greenland ice sheet. *J. Geophys. Res.* **119,** 631–645 (2014).
14. Xu, Y., Rignot, E., Fenty, I., Menemenlis, D. & Mar Flexas, M. Subaqueous melting of Store Glacier, West Greenland from three-dimensional, high-resolution numerical modeling and ocean observations. *Geophys. Res. Lett.* **40,** 4648–4653 (2013).
15. Christoffersen, P. *et al.* Warming of waters in an East Greenland fjord prior to glacier retreat: Mechanisms and connection to large-scale atmospheric conditions. *Cryosphere* **5,** 701–714 (2011).
16. Straneo, F. *et al.* Impact of fjord dynamics and glacial runoff on the circulation near Helheim Glacier. *Nature Geosci.* **4,** 322–327 (2011).
17. Johnson, H. L., Münchow, A., Falkner, K. K. & Melling, H. Ocean circulation and properties in Petermann Fjord, Greenland. *J. Geophys. Res.* **116,** C01003 (2011).
18. Enderlin, E. M. *et al.* An improved mass budget for the Greenland ice sheet. *Geophys. Res. Lett.* **41,** 866–872 (2014).
19. Straneo, F. *et al.* Characteristics of ocean waters reaching Greenland's glaciers. *Ann. Glaciol.* **53,** 202–210 (2012).
20. Sutherland, D. A. & Pickart, R. S. The East Greenland coastal current: Structure, variability, and forcing. *Prog. Oceanogr.* **78,** 58–77 (2008).
21. Schjøth, F. *et al.* Campaign to map the bathymetry of a major Greenland fjord. *EOS Trans. Am. Geophys. Union* **93,** 141–142 (2012).
22. Sutherland, D. A. *et al.* Atlantic water variability on the SE Greenland continental shelf and its relationship to SST and bathymetry. *J. Geophys. Res.* **118,** 847–855 (2012).
23. Harden, B. E., Renfrew, I. A. & Petersen, G. N. A climatology of wintertime Barrier winds off Southeast Greenland. *J. Clim.* **24,** 4701–4717 (2011).
24. Mernild, S. H. *et al.* Freshwater flux to Sermilik Fjord, SE Greenland. *Cryosphere* **4,** 453–465 (2010).
25. Stigebrandt, A. A mechanism governing the estuarine circulation in deep, strongly stratified fjords. *Estuar. Coast. Shelf S* **13,** 197–211 (1981).
26. Klinck, J. M., O'Brien, J. J. & Svendsen, H. Simple model of fjord and coastal circulation interaction. *J. Phys. Oceanogr.* **11,** 1612–1626 (1981).
27. Stigebrandt, A. On the response of the horizontal mean vertical density distribution in a fjord to low-frequency density fluctuations in the coastal water. *Tellus A* **42,** 605–614 (1990).
28. Arneborg, L. Turnover times for the water above sill level in Gullmar Fjord. *Cont. Shelf Res.* **24,** 443–460 (2004).
29. Holland, P. R., Jenkins, A. & Holland, D. M. The Response of ice shelf basal melting to variations in ocean temperature. *J. Clim.* **21,** 2558–2572 (2008).
30. Amundson, J. M. *et al.* Ice mélange dynamics and implications for terminus stability, Jakobshavn Isbræ, Greenland. *J. Geophys. Res.* **115,** F01005 (2010).

Acknowledgements

We acknowledge funding support from NSF and Woods Hole Oceanographic Institution's Ocean Climate Change Institute and logistical support from Greenpeace International. We would like to thank S. Lentz, G. Hamilton, L. Stearns, W. Ostrom, J. Kemp, A. Ramsey and D. Torres for their help.

Author contributions

F.S. and D.A.S. conceived the study. F.S., D.A.S. and R.H.J. carried out the fieldwork. R.H.J. processed and analysed the data. R.H.J., F.S. and D.A.S. interpreted the results. R.H.J. wrote the paper.

Additional information

Supplementary information is available in the online version of the paper. Reprints and permissions information is available online at www.nature.com/reprints. Correspondence and requests for materials should be addressed to R.H.J.

Competing financial interests

The authors declare no competing financial interests.